

Proceedings of the 47th International School and Conference on the Physics of Semiconductors “Jaszowiec 2018”

XPS Study of Te-protected Surface of $\text{Sn}_{1-x}\text{Mn}_x\text{Te}$ Topological Crystalline Insulator

I.N. DEMCHENKO^{a,*}, Y. SYRYANYI^b, M. ZIEBA^{a,†}, R. MINIKAYEV^a, E. ŁUSAKOWSKA^a,
M. WIATER^a, P. KONSTANTYNOV^a, T. WOJTOWICZ^c AND T. STORY^a

^aInstitute of Physics, Polish Academy of Sciences, Aleja Lotników 32/46, PL-02668 Warsaw, Poland

^bFaculty of Chemistry, Biological and Chemical Research Centre UW,
Żwirki i Wigury 101, PL-02689 Warsaw, Poland

^cInternational Research Centre MagTop, Institute of Physics, Polish Academy of Sciences,
Aleja Lotników 32/46, PL-02668 Warsaw, Poland

We present X-ray photoelectron spectroscopy studies of epitaxial layers of $\text{Sn}_{0.95}\text{Mn}_{0.05}\text{Te}/\text{CdTe}/\text{GaAs}(001)$ — a ferromagnetic topological crystalline insulator. We demonstrate that by terminating the molecular beam epitaxy growth of the layer with 20 nm crystalline Te cap one can protect the layer against oxidation at ambient conditions and, after short thermal annealing in X-ray photoelectron spectroscopy chamber, obtain atomically clean (001) surface of high crystal quality, suitable for angle-resolved photoelectron spectroscopy studies of surface topological states.

DOI: [10.12693/APhysPolA.134.937](https://doi.org/10.12693/APhysPolA.134.937)

PACS/topics: 73.20.At, 75.50.Pp, 82.80.Pv

1. Introduction

SnTe as well as related substitutional solid solutions $\text{Pb}_{1-x}\text{Sn}_x\text{Te}$ and $\text{Pb}_{1-x}\text{Sn}_x\text{Se}$ are IV–VI semiconductors recently recognized as topological crystalline insulators (TCI). In these new topological materials with an inverted band ordering the mirror-plane crystalline symmetry protects surface electronic states with the Dirac-like energy dispersion. Following theoretical proposal [1] the experimental discovery was done with angle-resolved photoelectron spectroscopy (ARPES) method applied to atomically clean (001) surfaces obtained by cleaving the crystals in ultrahigh vacuum [2–4]. This simple and versatile method cannot be used for many important topological systems, e.g. multilayer heterostructures or poorly cleaving bulk materials, like lead and tin tellurides. Therefore, developing the methods of analyzing, modifying and protecting the surface of TCI layers is a research task vital for future development of this field towards functional electronic and optical heterostructures.

SnTe is a diamagnetic material that after incorporation of Mn magnetic ions, thus forming a diluted magnetic (semimagnetic) semiconductor solid solution $\text{Sn}_{1-x}\text{Mn}_x\text{Te}$, exhibits the carrier-induced ferromagnetism [5–7]. An interplay of topological and ferromagnetic properties of $\text{Sn}_{1-x}\text{Mn}_x\text{Te}$ constitutes a new field of research. As the growth of bulk $\text{Sn}_{1-x}\text{Mn}_x\text{Te}$ monocrystals with good cleaving properties is very challenging, we

use thick epitaxial layers of $\text{Sn}_{1-x}\text{Mn}_x\text{Te}$ with removable Te capping for transportation between growth facilities and external experimental setups equipped with suitable UHV preparation chamber that permits annealing treatment. This approach was recently successfully tested for nonmagnetic $\text{Pb}_{1-x}\text{Sn}_x\text{Te}$ and $\text{Pb}_{1-x}\text{Sn}_x\text{Se}$ IV–VI topological substitutional alloys [8]. However, the incorporation of Mn ions in IV–VI materials — a necessary step in preparing magnetic TCI materials — brings an important problem of possible formation of several known Mn oxides or tellurides. Mn ions chemically bound in these compounds would not participate in the formation of ferromagnetic state as this requires substitutional Mn^{2+} ions coupled by p – d exchange interaction to conducting holes [5–7]. In this work we present our findings obtained by conventional X-ray photoelectron spectroscopy (XPS) study of $\text{Sn}_{1-x}\text{Mn}_x\text{Te}$ epitaxial layers protected from oxidation with very thin tellurium cap.

2. Experimental

$\text{Sn}_{1-x}\text{Mn}_x\text{Te}$ ($x = 0.05$) layers were grown by molecular beam epitaxy (MBE) using effusion cells with compound (SnTe) and elemental (Mn and Te) sources. As the substrate GaAs (001) wafer with 0.5° miscut overgrown by CdTe thick (4 μm) buffer layer was used. The growth process of $\text{Sn}_{1-x}\text{Mn}_x\text{Te}$ was carried out at substrate temperature of about 350°C and, after reducing the substrate temperature to 25°C , it was terminated with deposition of 20 nm thick Te cap. The $\text{Sn}_{1-x}\text{Mn}_x\text{Te}$ layers were covered by either amorphous (a-Te) or crystalline (c-Te) capping layer. The growth of the layers and the cap was monitored *in situ* by reflection high energy electron diffraction (RHEED) method. The layer prepared in such a way was transferred in ambient air environment

*corresponding author; e-mail: demch@ifpan.edu.pl

†corresponding author; e-mail: zieba@ifpan.edu.pl

into ultra-high vacuum system of the XPS facility where it was subjected to various annealing procedures. The XPS, atomic force microscopy (AFM), and X-ray diffraction (XRD) methods were applied to investigate the electronic structure, chemical composition, and structural properties of the (001) surface of $\text{Sn}_{1-x}\text{Mn}_x\text{Te}$ layer. The XPS and low-energy electron diffraction (LEED) data were acquired in an UHV Scienta/Prevac spectrometer system described previously in Ref. [9]. The XPS studies were performed using a monochromatic Al K_α radiation ($h\nu = 1486.6$ eV) from an X-ray source (ScientaVG, MX650) irradiating a spot size of 6×2 mm². The high resolution (HR) XPS spectra were collected with the hemispherical analyzer (ScientaVG R4000) at 0° (60°) take-off angle to the surface's normal with a pass energy of 200 eV and an energy step size of 0.15 eV. Let us note that for the used spectrometer a set-up FWHM of Ag $3d$ line is < 0.58 eV. Binding energies (BE) of the photoelectrons were calibrated using gold $4f_{7/2}$ line (84 eV). The CasaXPS software (version 2.3.17) was used to evaluate the XPS data [10]. The LEED images were recorded with a fluorescence screen. The primary electron beam voltage was 100 eV. The heat treatment was performed in a vacuum of 10^{-9} mbar up to $T = 250\text{--}290$ °C for 20 min duration. These temperature/time limits were set based on previous RHEED investigations.

3. Results

The good quality of crystal structure of $\text{Sn}_{1-x}\text{Mn}_x\text{Te}$ layers with Te cap was confirmed by XRD investigations. The $\omega/2\theta$ scans revealed sharp Bragg peaks of the zinc-blende GaAs/CdTe (001) substrate and the rock-salt $\text{Sn}_{1-x}\text{Mn}_x\text{Te}$ (001) layer as well as additional peaks due to (101) oriented tellurium cap. Next, Te-capped $\text{Sn}_{1-x}\text{Mn}_x\text{Te}$ samples had been reintroduced into vacuum chamber and were checked by XPS (see Figs. 1, 2: before annealing (BA)) and then annealed at 250–290 °C for 20 min to decap the pure tellurium layer. The temperature was measured with a thermocouple attached to the sample holder. Following this process, LEED patterns, such as the one shown on the inset in Fig. 1 (bottom), revealed the $\text{Sn}_{1-x}\text{Mn}_x\text{Te}$ (001) crystal surface while the XPS spectra confirmed that the tellurium cap layer was entirely removed.

Let us discuss the results for Te and Sn $3d$ lines represented in Figs. 1, 2 in more details. The presented data are background subtracted and normalized to the maximum of Te $3d_{5/2}$ and Sn $3d_{5/2}$ peak intensity, for clarity. It should be noticed that in the sample 2 after the annealing treatment, the manganese $2p$ line was also registered (BE: $\approx 640.90 \pm 0.15$ eV corresponding to Mn^{2+} in MnTe-like semiconductor materials [11]). Due to the low statistics of these data and the fact that investigation of these electron states is out of the scope of this short paper we do not present them here.

Before the annealing treatment one can distinguish two distinctive components for sample 1 corresponding to the metallic tellurium, Te^0 (BE: 572.92 ± 0.15 eV), and Te in

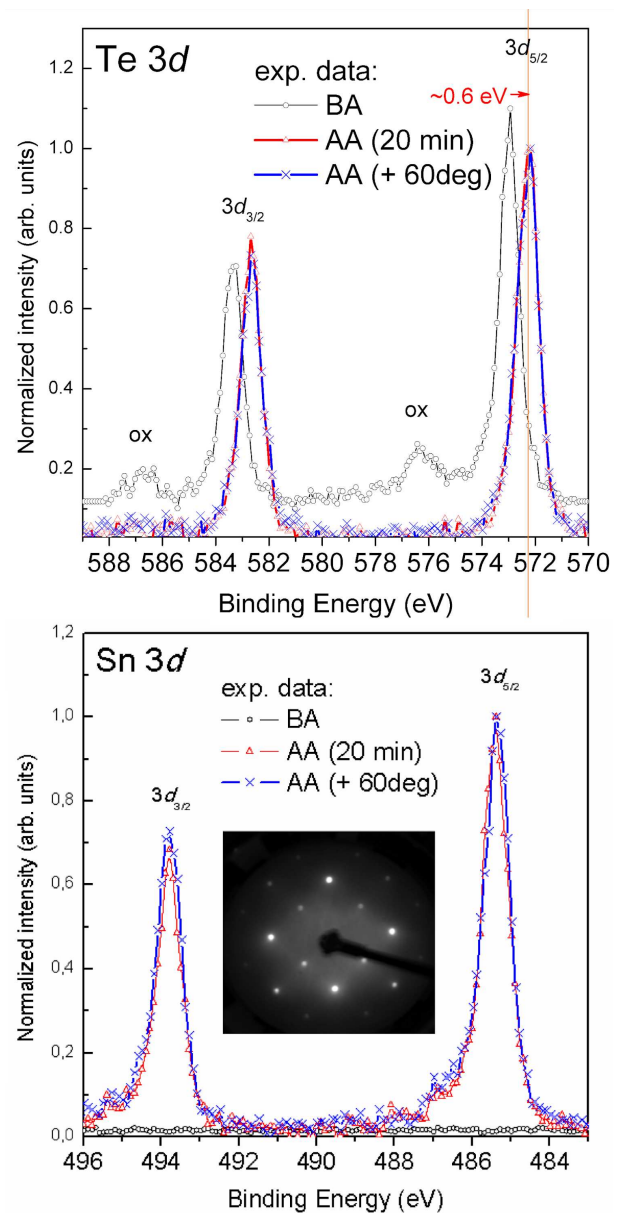


Fig. 1. XPS spectra for sample 1 ($\text{Sn}_{1-x}\text{Mn}_x\text{Te}$ covered by c-Te thin film): (top) Te $3d$ states before annealing (BA, 0° take off angle), after 20 min annealing (AA) with 60° take off angle; (bottom) Sn $3d$ states with the same conditions like above. In the inset of the bottom figure the LEED pattern of the annealed $\text{Sn}_{1-x}\text{Mn}_x\text{Te}$ (001) surface is shown.

tellurium oxide (BE of $3d_{5/2}$: 576.40 ± 0.15 eV; marked “ox” in Fig. 1 (top)). The observed “chemical shift” is an effective indicator of the charge transfer between O $2p$ and Te $3d$ states. Before annealing, signal that corresponds to Sn (see Fig. 1 (bottom, black opened circles)), is not visible making clear that signal is collected from c-Te cap layer only. The Te $3d_{5/2}$ line is shifted to higher BE for ≈ 0.6 eV as a result of annealing process. Estimated BE of Te $3d_{5/2}$ line is 572.28 ± 0.15 eV corresponding to the anion state, i.e. Te^{2-} in SnTe and is identi-

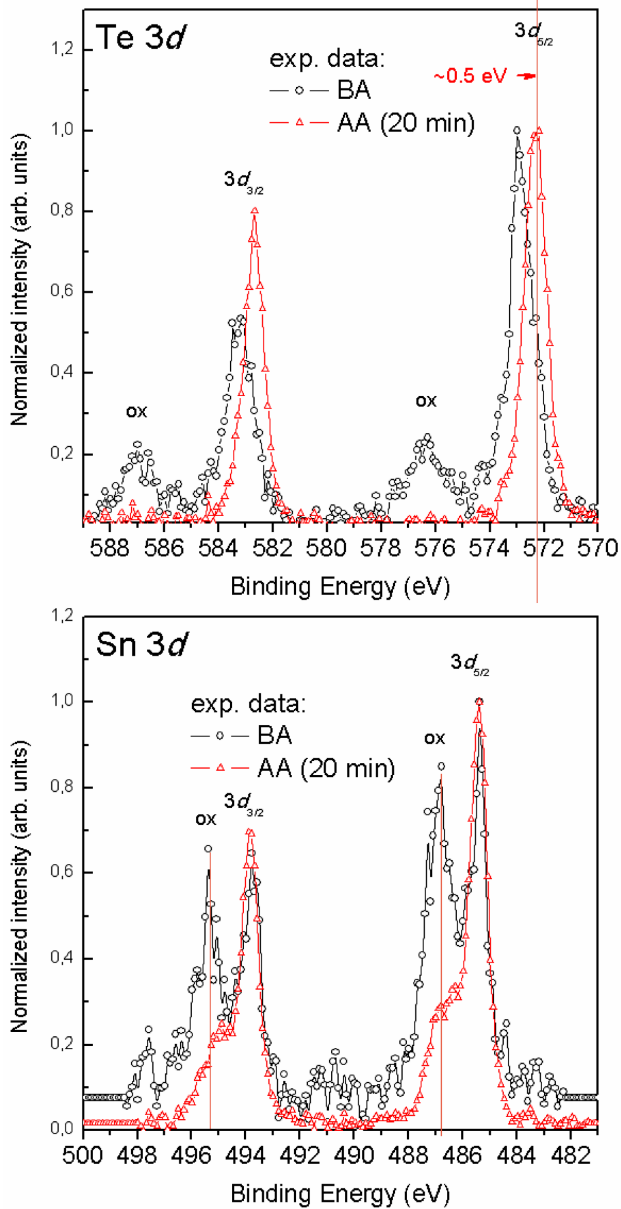


Fig. 2. XPS spectra for sample 2 ($\text{Sn}_{1-x}\text{Mn}_x\text{Te}$ covered by a-Te thin film): (top) Te 3d states before annealing (BA, 0° take off angle), after 20 min annealing (AA, 0° take off angle); (bottom) Sn 3d states with the same conditions like above.

cal with the ones reported by Shalvoy et al. [12]. An important observation is that oxygen component, thus Te-oxide/s, is absent here. Such an observation is true also for Sn 3d (see Fig. 1: bottom, after annealing (AA) treatment). To concentrate more on the topmost surface, extra measurements were done. XPS signal was gathered in angle resolved regime (with photoelectrons “take off” angle of 60° (details of such measurements could be found, for instance, in Ref. [9])). For that geometry Sn 3d states revealed minor contribution of oxygen bonded to tin atoms (at level $\leq 1\%$). Consequently, minor part of tin atoms at the surface is oxidized, despite the remain-

ing tellurium at the surface which does not react with oxygen. The authors suggest that the observed oxygen originates from contamination. As it is well known, the main source of contamination in the vacuum system is the residual gas. From the molecular-kinetic theory of gases, the number of particles striking the sample surface could be presented in the following form:

$$n_s = N \left(\frac{RT_a}{2\pi M} \right)^{1/2} \approx \sqrt{3.5 \times 10^{22} \left(\frac{p}{MT_a} \right)^{1/2}}$$

where R is the gas constant, T_a is the absolute temperature, M is the molecular weight, p is the gas pressure in Torr. Consequently, if it is assumed that a monolayer contains 3×10^{14} particles/cm², the average molecular weight is $M = 28$, and $T_a = 300$ K, we obtain $n_s = 10^6$ p. This means that at the pressure of 10^{-6} Torr, the number of molecules per second is enough to form a monolayer. Following this explanation and taking into account working pressure during the XPS experiment and time needed for the data collection (a few hours per one examined photoelectron line), we can conclude that the observed oxygen is a contamination at $\text{Sn}_{1-x}\text{Mn}_x\text{Te}$ surface. Such an explanation is not applicable for sample 2, where Sn-oxide contribution is significant both before and after the annealing treatment (see Fig. 2 (bottom)).

The behaviour of the Te 3d line (before and after the annealing procedure) for sample 2, coated with amorphous tellurium, is quite similar to sample 1 (see Figs. 1 and 2). Opposite is true for Sn 3d photoelectron peak, where contribution of Sn^{2+} cationic state, BE is 485.34 ± 0.15 eV, close to the BE in SnTe [11, 13], goes together with a signal from the Sn-oxide (marked “ox” in Fig. 2). Following annealing the intensity of this signal decreases, but even then, the content of Sn-oxide fraction is considerable. It is important to note that signal of Sn 3d line in sample 2, compared as opposite to the case of sample 1 is visible even before annealing treatment. This observation allowed suggesting that a-Te cap layer grown on the $\text{Sn}_{1-x}\text{Mn}_x\text{Te}$ interface is in the form of non-coalescing tellurium islands (with thickness < 10 nm). This hypothesis was finally confirmed by AFM measurements (data are not presented here). Consequently, opened spaces between these islands enabled the more chemically active tuning $\text{Sn}_{1-x}\text{Mn}_x\text{Te}$ layer to bound with oxygen in the atmospheric conditions (i.e. during transfer of the samples to UHV chamber).

4. Conclusions

The method for preparing a clean surface of MBE grown layer of topological crystalline insulator, $\text{Sn}_{1-x}\text{Mn}_x\text{Te}$, was investigated by XPS spectroscopy. It was found that cleaning by the temperature annealing at $250\text{--}290^\circ\text{C}$ for 20 min removed the oxidized crystalline c-Te cap layer (sample 1), making ARPES measurements of surface electronic states possible. It was also found that due to different growth mode and different surface morphology observed by AFM in sample 2 deposition of a thin amorphous layer (< 10 nm) a-Te was not enough

to cover whole surface of $\text{Sn}_{1-x}\text{Mn}_x\text{Te}$ layer. As a result, the a-Te cap layer in the investigated sample was not sufficient to protect TCI surface and huge fraction of Sn bonded to oxygen was clearly seen. The procedure developed and studied here provides a very simple access to atomically clean (001) topological surfaces of MBE-grown ferromagnetic TCI materials based on $\text{Sn}_{1-x}\text{Mn}_x\text{Te}$ without necessity of using destructive ion sputtering.

Acknowledgments

This work was partially supported by the National Science Centre (Poland) research project 2014/15/B/ST3/03833 and by the Foundation for Polish Science through the IRA Programme co-financed by EU within SG OP.

References

- [1] T. H. Hsieh, H. Lin, J. Liu, W. Duan, A. Bansil, L. Fu, *Nature Commun.* **3**, 982 (2012).
- [2] Y. Tanaka, Z. Ren, T. Sato, K. Nakayama, S. Souma, T. Takahashi, K. Segawa, Y. Ando, *Nature Phys.* **8**, 800 (2012).
- [3] P. Dziawa, B. J. Kowalski, K. Dybko, R. Buczko, A. Szczerbakow, M. Szot, E. Łusakowska, T. Balasubramanian, B.M. Wojek, M.H. Berntsen, O. Tjernberg, T. Story, *Nature Mater.* **11**, 1023 (2012).
- [4] S.-Y. Xu, C. Liu, N. Alidoust, M. Neupane, D. Qian, I. Belopolski, J.D. Denlinger, Y.J. Wang, H. Lin, L.A. Wray, G. Landolt, B. Slomski, J.H. Dil, A. Marcinkova, E. Morosan, Q. Gibson, R. Sankar, F.C. Chou, R.J. Cava, A. Bansil, M.Z. Hasan, *Nature Commun.* **3**, 1192 (2012).
- [5] P.J.T. Eggenkamp, H.J.M. Swagten, T. Story, V.I. Litvinov, C.H.W. Swüste, W.J.M. de Jonge, *Phys. Rev. B* **51**, 15250 (1995).
- [6] A.J. Nadolny, J. Sadowski, B. Taliashvili, M. Arciszewska, W. Dobrowolski, V. Domukhovski, E. Łusakowska, A. Mycielski, V. Osinniy, T. Story, K. Świątek, R.R. Gałazka, R. Diduszko, *J. Magn. Magn. Mater.* **248**, 134 (2002).
- [7] T. Story, P.J.T. Eggenkamp, C.H.W. Swüste, H.J.M. Swagten, W. J. M. de Jonge, A. Szczerbakow, *Phys. Rev. B* **47**, 227 (1993).
- [8] V.V. Volobuev, P.S. Mandal, M. Galicka, O. Caha, J. Sánchez-Barriga, D. Di Sante, A. Varykhalov, A. Khair, S. Picozzi, G. Bauer, P. Kacman, R. Buczko, O. Rader, G. Springholz, *Adv. Mater.* **29**, 1604185 (2017).
- [9] I.N. Demchenko, Y. Syryanyy, Y. Melikhov, L. Nittler, L. Gladczuk, K. Lasek, L. Cozzarini, M. Dalmiglio, A. Goldoni, P. Konstantynov, M. Chernyshova, *Scr. Mater.* **145**, 50 (2018).
- [10] Software package for the analysis of XPS results, CasaXPS version 2.3.17dev6.6o.
- [11] R.J. Iwanowski, M.H. Heinonen, W. Paszkowicz, R. Minikaev, T. Story, B. Witkowska, *Appl. Surf. Sci.* **252**, 3632 (2006).
- [12] R.B. Shalvoy, G.B. Fisher, P.J. Stiles, *Phys. Rev. B* **15**, 1680 (1977).
- [13] N. Berchenko, R. Vitchev, M. Trzyna, R. Wojnarowska-Nowak, A. Szczerbakow, A. Badyła, J. Cebulski, T. Story, *Appl. Surf. Sci.* **452**, 134 (2018).